ANALYSIS OF STELLAR WIND STRUCTURE OF MASSIVE STAR THROUGH THEIR X-RAY SPECTRA

A. Hervé[1]

Abstract. Massive stars play a key role in the chemical enrichment of the universe. At the end of 90's, the evidence of fragmented wind have been highlighted thanks to observations as well as spectra simulation. During the same time, two X-ray space observatories were launched, opening a new window for the massive star stellar wind analyses.

In this context, we are currently developing a modelling tool to analyse the stellar wind structure as well as a determination of fundamental properties of massive star like mass loss rate and surface abundances thanks to their X-ray spectra.

Our results, with our code, have revealed the absence of porosity of the stellar wind (i.e even through stellar winds are fragmented the space between clumps is thin.) of ζ Pup and ζ Ori. For the first time, we have determined the temperature distribution of the X-ray emitting plasma. The highest temperatures are localized in very thin shells (~ 1. R_*) at few stellar radius. The lowest temperatures are discovered in very extended shells and the X-ray emission can arise very close to the stellar surface (1.3-1.5 R_*). Finally, we determined CNO abundances and mass loss rate in agreement with previous UV/visible studies.

Keywords: Stars: early-type, Stars: mass-loss, X-rays: stars, Stars: massive, Stars: individual: ζ Pup ζ Ori

1 Introduction

Massive stars are the main agents of the chemical enrichment of galaxies. Due to their high temperature they can synthesize the heaviest elements during their different evolution phases. They release these elements in their local environment during all their life through their powerful stellar winds and at lager scale at the end of their life during supernovae explosion.

At the end of the 90's, some observational studies revealed that some time variability of the spectrum of star is due to the presence of fragmentation (Eversberg et al. 1998). Our traditional point of view of homogeneous stellar winds has evolved to fragmented structures. The implementation of the clumping in modelling code (Bouret et al. 2005) has improved the fitting. But, in consequence the mass loss rate has been divided by a factor between 3 and 10. This huge reduction has consequence on the evolution scheme of the massive star.

In 1999, two X-ray spectrographes were launched, $XMM - Newton$ and *Chandra*. These two instruments have opened a new window to analyse the stellar wind properties of the massive stars. The scientific community can now access to high resolution spectra of massive star in the X-ray band. In these context, we are currently developing and improving a modelling tool which allow us to understand the line formation in the X-ray band and to extract fundamental parameters of massive stars.

We present, in the section 2, our modelling code and the basics of physics included. Then, in the section 3, we present the results obtained by the analyses of X-ray spectra of ζ Pup and ζ Ori. Finally, in the last section, we discuss these results and their impacts in our knowledge of the massive stars.

---

[1] LUPM, Université Montpellier II, Place Eugène Bataillon, F-34095 MONTPELLIER Cedex 05, France

2   Modelling tool

We are currently developing our own modelling tool in order to analyse high resolution spectra of O-type stars and to determine their stellar wind properties (Hervé et al. (2012); Hervé et al. (2013), Hervé et al, in prep). The code is decomposed in two different parts. First, the code computes synthetic X-ray spectra as a function of different input parameters like the mass loss rate, the surface chemical abundances, and the temperature, the position and the size of the X-ray emitting shell. Then, a second routine combines different X-ray synthetic spectra in order to reproduce observations.

In our code, the X-ray photons production is based on the wind embedded shock scenario. The strong instabilities in the wind drive to collisions, heating plasma to very high temperatures (1-10 10^6 K). Then, this heated matter is embedded by the 'cool' material. In our approach, we consider that the X-ray emitting plasma is optically thin to X-ray. Consequently, we can compute the emission and the absorption separately. So, in a first part, we calculate the X-ray theoretical emission of a shell as a function of its density and of the theoretical emissivity of the plasma. For the latter, we use the AtomDB database (Foster et al. 2012). Then we have modified the Owocki formalism (Owocki & Cohen 2006) to determine the absorption of X-ray photon by the cool material. Now, we include the wavelength and the radial dependence of the mass absorption coefficients, κ, as keeping an analytic solution of the optical depth equation to compute synthetic models fast:

$$
\begin{aligned}
\tau_\lambda(p,z) &= \int_z^{\sqrt{(R_{lim})^2 - p^2}} \frac{\alpha(\kappa_0 - \gamma R_*)R_*}{r'\,(r' - R_*) + \alpha\,(\kappa_0 + \gamma(r' - R_*))\,h'\,r'}\,dz' \\
&+ \int_z^{\sqrt{(R_{lim})^2 - p^2}} \frac{\alpha\gamma R_*}{(r' - R_*) + \alpha(\kappa_0 + \gamma(r' - R_*))h'}\,dz' + \int_{\sqrt{(R_{lim})^2 - p^2}}^{\infty} \frac{\alpha\kappa_{max}R_*}{r'\,(r' - R_*) + \alpha\kappa_{max}h'\,r'}\,dz'
\end{aligned}
$$

with $\alpha = \frac{\dot{M}}{4\pi R_* v_\infty}$, κ_0 and κ_{max} are, respectively, the mass absorption coefficient in the innermost part and in the outer part of the wind and γ is the slope. R_{lim} is the position in the wind where κ reaches its plateau value κ_{max}. h' is the porosity length. To determine $\kappa(\lambda, r)$, we use the radiative code CMFGEN (Hillier & Miller 1998). This code solves the radiative transfer equation and statistical equilibrium equations for each ions in Non Local Thermodynamical Equilibrium (NLTE) conditions as a function of stellar and wind parameters. Finally, we combine the emission and the absorption components to obtain a synthetic spectrum.
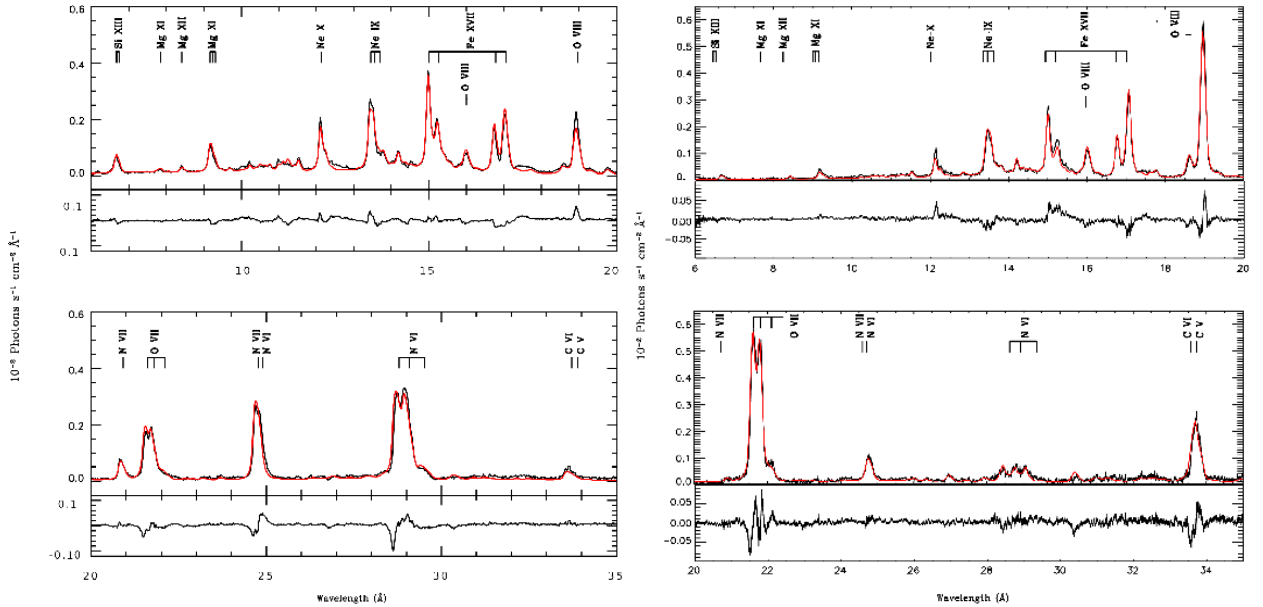

Fig. 1. Left: Comparison of our best fit model (in red) to the RGS spectrum of ζ Pup (in black). Right: Comparison of our best fit model (in red) to the RGS spectrum of ζ Ori. The residuals (in the sense observation minus model) are shown in the panel under the spectra.

In the second part of the code, a fitting routine explores a database of synthetic models, and combines different plasma components with the same chemical composition, h' and $\dot{M}$ in order to fit the observation.

kT in keV	R_{in} in R_*	R_{out} in R_*	hot gas filling factor f_X
0.100	7.5	85	0.012
0.200	1.5	38	0.012
0.400	2.7	4.0	0.020
0.690	3.1	4.1	0.007

Table 1. X-ray temperature distribution in the wind of ζ Pup

The synthetic multi-temperature spectrum is built as follows:

$$S_i = \sum_{j=1}^{n} \sum_{r=R_{in}}^{R_{out}} f_{hotgas,j,r} M_{j,i,r} + \epsilon, \qquad (2.1)$$

where S_i is the observed flux at the wavelength i, $f_{hotgas,j,r}$ is the classical volume filling factor of the hot gas component j at the position r, $M_{j,i,r}$ is the synthetic flux of each X-ray emitting plasma component at the wavelength i at the position r, and ϵ is the error of regression. Note that the analysis of ζ Pup was made with a previous version of our code and the radial dependence of f was not included yet.

For each combination of synthetic models, the best-fit values of $f_{hotgas,j}$ are determined with a non negative least-squares algorithm. Then, we calculate the χ^2 by comparing the model to the data. Finally, a minimisation of the χ^2 is performed to obtain the best fit. After several tests, it appears that at least four components are needed to achieve a good fit of the whole fluxed RGS spectra of ζ Pup and ζ Ori.

3   Results

We applied our code to ζ Pup (Nazé et al. 2012; Hervé et al. 2013) and ζ Ori (Hervé et al in prep) which are the two XMM most observed O-type stars. For the first time, we have fitted X-ray spectra as a whole and not like the traditional line-by-line analysis. The results are very good as show in Fig.1. A discrete decomposition of the X-ray emitting plasma in four temperature components from 0.1 keV to 0.690 keV allow us a better understanding of the distribution of the shocks in these stars (Tab.1). In the both case, we found that the hottest temperatures are localized in small shells ($R_{shell} = 1 - 2R_*$) at very few stellar radii ($R_0 \sim 2.5 - 3.5R_*$). The intermediate temperature shell is a little bit larger than the hottest one ($R_{shell} = 1.5 - 2.5R_*$) and localized a little bit closer to the stellar surface ($R_0 \sim 2. - 3R_*$). The two lowest temperature components are different. In the case of ζ Pup, we considered only one shell at a give temperature. Large emitting shells ($R_{shell} = 77.5R_*, 36.5R_*$, for the 0.1 keV and 0.2 keV respectively) are detected. The coolest component starting to emits at large radii ($R_0 = 7.5R_*$) while the component at 0.2 keV starts to emit very close to the stellar surface ($R_0 = 1.5R_*$). In the case of ζ Ori, with the first version of the code, we obtained too much flux in the blue part of the lines produced by the shell with the coolest temperature plasma. The utilization of the porosity to increase the flux in the red part (Owocki & Cohen 2006; Hervé et al. 2012) did not improved the quality of the fit. Consequently, we have modified our code which now takes into account a possible non-continuous emission of X-ray photons of a given shell at a given temperature as well as a possible radial dependence of f. With this new method, we have improved the quality of the fit. We discovered the presence of a small shell very close to the stellar surface ($R_0 = 1.2 - 1.3R_*$). The same shell is may be present in the wind of ζ Pup but as the wind is denser than the wind of ζ Ori, all the photons emit by this shell are totally absorbed by the 'cool' matter component. Unfortunately, this new method leads to a degeneracy of the results. We obtained the same quality of fit with numerous small emitting shells with a huge value of f, or with large shells with a small value of f. We need theoretical constraints of f and/or the size of the emitting shells to break the degeneracy.

Concerning the stellar wind parameters (Tab.3), our code can allow us a determination of mass loss rate, wind structure (porous or homogeneous) and CNO abundances. Taking into account the different approximation in CMFGEN (used in visible and UV analyses) and in our code as well as the accuracy of the atomic data, our determination of the CNO abundances for ζ Pup and ζ Ori is very close to the result obtained in analyses in other wavelength band (Tab.3). For ζ Ori, we obtain solar abundances for the CNO elements as Martins et al. (2012) in their study in yhe visible band. Concerning ζ Pup, we obtain a depletion of carbon and oxygen and a over abundance of nitrogen as the result of Bouret et al. (2012) in their analyses in visible band. Nevertheless, the over abundance of Nitrogen found in our work is less important than in visible band work.

Table 2. Our best stellar wind parameters obtained for ζ Pup and ζ Ori in the X-ray band compared to UV/visible studies.

Object	study	$\dot{M}$ ($M_\odot$ yr^{-1})	X(C) (mass fraction)	X(N) (mass fraction)	X(O) (mass fraction)	h
ζ Ori	Hervé et al in prep in X-ray	$1.0\ 10^{-6}$	2.08×10^{-3}	4.45×10^{-4}	3.84×10^{-3}	0
	Martins et al. (2012)	$1.7\ 10^{-6}$	2.07×10^{-3}	2.96×10^{-4}	5.27×10^{-3}	*
ζ Pup	Hervé et al. (2013) in X-ray	$3.5\ 10^{-6}$	6.00×10^{-4}	7.70×10^{-3}	3.05×10^{-3}	0
	Bouret et al. (2012)	$2.\ 10^{-6}$	2.86×10^{-4}	1.02×10^{-2}	1.30×10^{-3}	*

A very important result from our analyses is that the wind of massive stars is not porous. Even though the UV and visible studies of ζ Pup and ζ Ori revealed a fragmented wind, our work reveals that the space between clumps is very thin. Moreover, the determination of the mass loss rate for the both stars in the different wavelength bands are in good agreement. The results obtained in the case of ζ Ori are very close and the small difference is certainly due to the error bar in the both works. In the case of ζ Pup, the difference of the mass loss rate is greater than in the case of ζ Ori, but Bouret et al. (2012) indicate in their paper that the mass loss rate is not enough powerful to support the line driving acceleration in the inner part. They supposed that the mass loss rate is certainly greater than the one they found for their best fit. This remark confirm our result obtained from the X-ray spectrum analysis.

4   Conclusions and Discussions

In conclusion, we have fitted for the first time the whole X-ray spectra of O-type stars. We found that the hottest temperature plasma shells are relatively thin and localized at few stellar radii. Concerning the shell with the lowest temperature plasma, the situation is more complicated. In the case of ζ Pup, we found a continuous emission of X-ray photon from extended shells, one close to the photosphere the other one at large radii. In the case of ζ Ori, our model predicts, with the first version, too much flux in the blue wing of the emission lines ($\lambda \geq 20$Å) produced by the cool temperature (kT=0.1 ,0.2 keV) plasma components. The solution to explain this phenomenon is not the porosity but the presence of a small low temperature X-ray emitting shell very close to the surface of the star ($R_0 \sim 1.2R_*$). But this result has also revealed a degeneracy of the solution. We have, now, a non continuous X-ray emission for each shell at a given temperature plasma and a radial dependence of the hot gas filling factor. We can fit with the same degree of satisfaction the data with numerous small shells associated to a huge f or few large shells with a small f. We need to better understand the cooling function of X-ray emitting plasma to constrain the size of the emitting shells and to break the degeneracy.

Finally, as expected, the stellar wind parameters determined in our X-ray analyses are in good agreement with the results obtained by other studies in different wavelength bands. The non solar abundances of the CNO elements of ζ Pup indicate that this object is a more evolved star than ζ Ori. The visible/UV works show a fragmentation of the stellar wind and our work indicate that the space between fragments is very thin.

References

Bouret, J.-C., Lanz, T., & Hillier, D.J. 2005, A&A 438, 301

Bouret, J.-C., Hillier, D. J., Lanz, T., & Fullerton, A. W. 2012, A&A, 544, A67

Eversberg, T., Lépine, S., & Moffat, A.F.J. 1998, ApJ 494, 799

Foster, A. R., Ji, L., Smith, R. K., & Brickhouse, N. S. 2012, arXiv:1207.0576

Hervé, A., Rauw, G., Nazé, Y., & Foster, A. 2012, ApJ, 748, 89

Hervé, A., Rauw, G., & Nazé, Y. 2013, A&A, 551, A83

Hillier, J., & Miller, E. 1998, *ApJ*, 496, 416

Martins, F., Escolano, C., Wade, G. A., et al. 2012, A&A, 538, A29

Najarro, F., Hanson, M.M., & Puls, J. 2011, A&A, 535, A32

Nazé, Y., Flores, C. A., & Rauw, G. 2012, A&A, 538, A22

Owocki, S.P., & Cohen, D.H. 2006, ApJ 648, 565